

Effect of Substitution on the Electrical Conductivity of $\text{LiM}_x\text{Mn}_{2-x}\text{O}_4$ ($\text{M} = \text{Cu}, \text{Mg}, \text{Zn}$)

Yasumasa Tomita,* Hiroshi Yonekura, and Kenkichi Kobayashi

Department of Materials Science and Chemical Engineering, Shizuoka University, 3-5-1 Johoku, Hamamatsu 432-8561

(Received February 28, 2002)

$\text{LiM}_x\text{Mn}_{2-x}\text{O}_4$ ($\text{M} = \text{Cu}, \text{Mg}$ and Zn ; $x \leq 0.5$) was synthesized and the variance of the crystal structure and the electrical conductivity due to the substitution were studied. The crystal structure was changed by substitution, and the lattice constants decreased with x in $\text{LiZn}_x\text{Mn}_{2-x}\text{O}_4$. Both Zn and Li ions occupied tetrahedral sites. The Li–O bond became longer and Mn–O became shorter with increasing the content. The electrical conductivity for Mg and Zn compounds decreased from $10^{-4} \text{ S cm}^{-1}$ to $10^{-7} \text{ S cm}^{-1}$ with an increase in the Mg and Zn content. In the Cu compound, the conductivity was not changed very much. The infrared spectra for the Mg and Zn compounds shifted with x , indicating that the Mn–O bond became shorter and the Li–O bond longer with an increase in x . An XPS study showed a conversion of Mn^{3+} to Mn^{4+} with increasing the Mg, Zn or Cu content in these compounds.

Recently, high-performance batteries have stirred up interest, and many battery types have been developed for commercial use. Rechargeable lithium-ion batteries have been studied, especially because they exhibit the highest specific energy among rechargeable batteries. Each component of Li batteries has been extensively developed for improving the capacity and cycle-ability. Transition metal oxides, such as LiCoO_2 , LiNiO_2 , and LiV_3O_8 , have been studied as positive electrodes for several years.^{1–3}

Spinel LiMn_2O_4 is used as a cathode material for rechargeable lithium batteries, and many studies have been carried out because of its low cost and low toxicity.^{4–6} This material has a three-dimensional tunnel structure, and shows a reversible intercalation of lithium ions. The main operating problem for LiMn_2O_4 is a capacity drop resulting from a structural distortion due to a Jahn–Teller effect of the Mn^{3+} ion; therefore, several dopants such as Co, Al, Ni, and Zn were added to reduce a Jahn–Teller distortion and to improve the rechargeability.^{7–10} In general, the electrical conductivity is affected by a small amount of the dopants. Therefore, the electrical conductivity is expected to change with the content of the dopants.

It was reported that LiMn_2O_4 is a small-polaron semiconductor, and that the mobility of e_g electrons on Mn^{3+} ions carries an activation energy.¹¹ An investigation of the electrical conduction is very important because it is one of the most essential functions for application as the cathode material. In this paper, the effects of substituting Mg, Cu and Zn for Mn on the structure and the electrical conduction in $\text{LiM}_x\text{Mn}_{2-x}\text{O}_4$ ($\text{M} = \text{Mg}, \text{Cu}$ and Zn ; $0 \leq x \leq 0.5$) are discussed.

Experimental

$\text{LiM}_x\text{Mn}_{2-x}\text{O}_4$ was prepared by reacting the required stoichiometric amounts of Li_2CO_3 , MgCO_3 , CuO , ZnO , and MnO_2 , respectively. The mixed powders were calcined at 750°C in air for 40 hours and slowly cooled down to room temperature. Powder X-ray diffraction patterns were recorded using $\text{Cu-K}\alpha$ radiation to

characterize the samples. The X-ray patterns of the samples showed a single-phase spinel compound. The structures of these samples were determined from X-ray data using the Rietveld method.¹² The AC conductivity was measured at 11 frequencies between 100 Hz and 100 kHz in a dry nitrogen atmosphere (YHP LCR meter 4274A). A complex-plane impedance analysis was carried out to obtain the bulk conductivity. IR spectra were recorded with 2 cm^{-1} resolution between 400 cm^{-1} and 4000 cm^{-1} using a DR-8060 (Shimadzu) spectrometer. X-ray photoelectron spectroscopic (XPS) measurements were performed to identify the chemical state of Mn.

Results and Discussion

Crystal Structure. Li ions occupy tetrahedral sites surrounded by O ions, and Mn ions occupy octahedral sites in the spinel LiMn_2O_4 compound. It was reported that Cu ions in $\text{LiCu}_{0.5}\text{Mn}_{1.5}\text{O}_4$ occupy the tetrahedral site as well as the octahedral site.¹³ For $\text{LiMg}_x\text{Mn}_{2-x}\text{O}_4$, the lattice constant decreased with increasing Mg content; its crystal structure belongs to a new space group at $x > 0.33$.¹⁴ In the case of $\text{LiZn}_x\text{Mn}_{2-x}\text{O}_4$ ($0 \leq x \leq 0.5$), substitution for the Mn ion caused a change in their crystal structures and their lattice constants varied with x , as follows. In the case of $\text{LiM}_x\text{Mn}_{2-x}\text{O}_4$ ($\text{M} = \text{Mg}$ and Cu ; $0 \leq x \leq 0.5$), their lattice constants varied with x due to substitution for Mn.

Figure 1 shows the powder X-ray diffraction patterns of $\text{LiZn}_x\text{Mn}_{2-x}\text{O}_4$ ($0 \leq x \leq 0.5$). A new peak appeared by Zn substitution, indicating that the Li, Zn, and Mn ions were ordered in octahedral 16d sites. The space group of $\text{LiZn}_x\text{Mn}_{2-x}\text{O}_4$ was found to be $P2_13$ from these XRD patterns. The $\{200\}$ and $\{220\}$ diffraction peaks at $2\theta = 21.7^\circ$ and 30.9° become larger with increasing Zn content, which suggests that Zn occupies the tetrahedral sites. The XRD patterns shown in Fig. 1 were analyzed by the Rietveld method in thorough consideration of these findings. The results of Rietveld analyses for $x = 0.5$ are shown in Fig. 2, and Table 1 summarizes the data ob-

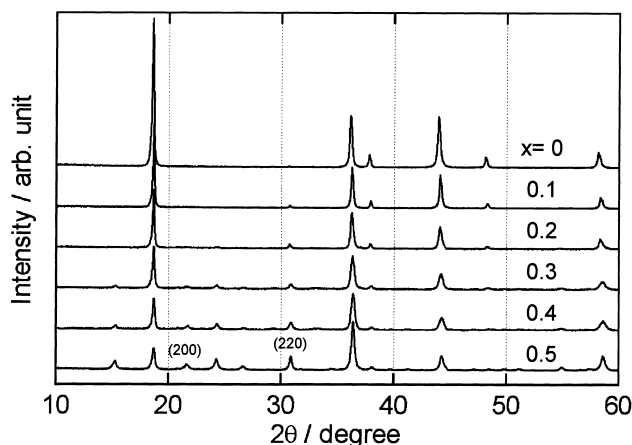


Fig. 1. Powder X-ray diffraction patterns of $\text{LiZn}_x\text{Mn}_{2-x}\text{O}_4$ ($0 \leq x \leq 0.5$) at 297 K.

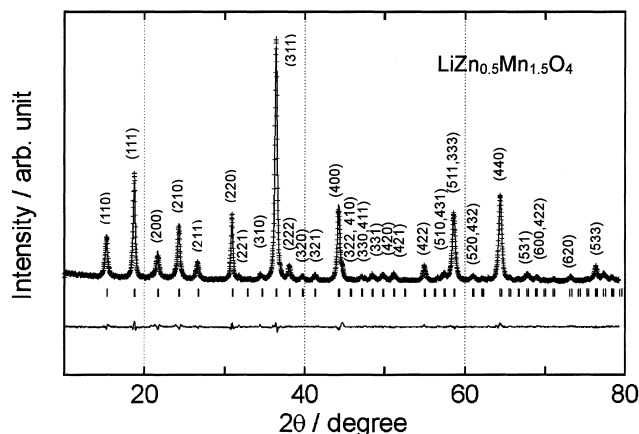


Fig. 2. The results of the Rietveld analysis of X-ray diffraction patterns for $\text{LiZn}_{0.5}\text{Mn}_{1.5}\text{O}_4$ at 297 K.

Table 1. Results of the Rietveld Analysis

Compound	Lattice constant/pm	R_{wp}	R_{p}
$\text{LiZn}_{0.1}\text{Mn}_{1.9}\text{O}_4$	821.19(3)	12.5	9.5
$\text{LiZn}_{0.2}\text{Mn}_{1.8}\text{O}_4$	820.38(4)	14.5	11.1
$\text{LiZn}_{0.3}\text{Mn}_{1.7}\text{O}_4$	819.27(4)	13.2	10.7
$\text{LiZn}_{0.4}\text{Mn}_{1.6}\text{O}_4$	818.78(4)	13.9	10.1
$\text{LiZn}_{0.5}\text{Mn}_{1.5}\text{O}_4$	818.16(3)	10.5	7.8

tained in the Rietveld analyses. The space group of LiMn_2O_4 was $Fd\bar{3}m$ based on analyses, and that of $\text{LiZn}_x\text{Mn}_{2-x}\text{O}_4$ was $P2_13$. R_{wp} , R_{F} and S ($= R_{\text{wp}}/R_{\text{F}}$) were within 15%, 5% and 1.3 in all of the analyses. The Zn and Li ions occupied the tetrahedral sites. $\text{LiZn}_x\text{Mn}_{2-x}\text{O}_4$ has two sorts of tetrahedral sites and the distributions of Zn and Li in both tetrahedral sites were found to be disordered. There are two sorts of octahedral sites, $4a$ and $12b$, in the $\text{LiZn}_x\text{Mn}_{2-x}\text{O}_4$; the $12b$ site is occupied only by Mn, and the $4a$ site is occupied by the remaining Mn and Li. In $\text{LiZn}_{0.5}\text{Mn}_{1.5}\text{O}_4$, the coordinates of the $4a$ and $12b$ octahedral site are (x, x, x) , $x = 0.634(1)$ and $(0.6290(5), 0.1317(4), 0.1363(4))$, respectively. Those of two $4a$ tetrahedral sites are $x = 0.003(1)$ and $0.243(1)$. The ratio of the each element obtained by handling the occupancy of each site inde-

pendently was in good agreement with the result from XPS measurements.

The lattice constants of $\text{LiZn}_x\text{Mn}_{2-x}\text{O}_4$ are summarized in Table 1, and gradually decrease with increasing x , similar to those of Cu and Mg compounds. The ionic radius of the Mn^{3+} ion is smaller than that of the Zn^{2+} , Mg^{2+} and Cu^{2+} ions,¹⁵ and the lattice constants of their compounds were estimated to be larger than that of the original LiMn_2O_4 . The substitution of the bivalent cation, however, causes an increase of the amount of Mn^{4+} ion, whose ionic radius is smaller than that of Mn^{3+} . Therefore, the lattice constants were decreased by substitution of those bivalent cations. The bond lengths were varied with x in each compound.

FT-IR Spectroscopy. Figure 3 shows the x dependence of the Fourier transformation infrared (FT-IR) spectra between 400 cm^{-1} and 800 cm^{-1} for LiMn_2O_4 and $\text{LiM}_x\text{Mn}_{2-x}\text{O}_4$ (Mg and Cu). Each spectrum consisted of two bands whose center wave numbers were ca. 620 and 525 cm^{-1} . According to previous papers,^{16–18} the peaks between 614 and 633 cm^{-1} and between 510 and 513 cm^{-1} are attributed to asymmetric stretching modes of the octahedral MnO group. On the other hand, a peak of the tetrahedral LiO group is expected to appear between 500 and 550 cm^{-1} .¹⁹ Therefore, the observed peak at 525 cm^{-1} is an overlapping of the LiO and MnO vibration peak. No significant changes were observed, and some of these bands shifted slightly following an increase in the amounts of substitution. In Mg and Zn compounds, the substitutions shift the positions of the band at 525 cm^{-1} to a lower wave number; in contrast another band at 614 cm^{-1} is shifted to higher wave numbers. A Rietveld analysis of the XRD patterns indicate that the Mn–O bond becomes shorter and Li–O

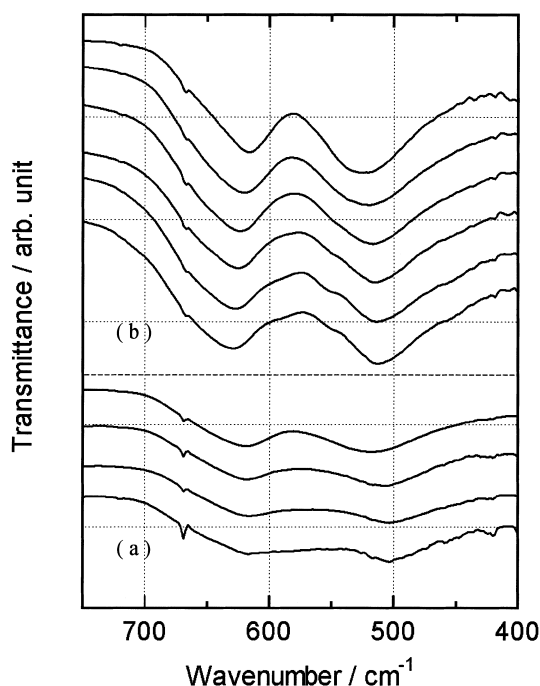


Fig. 3. x dependence of FT-IR spectra for $\text{LiM}_x\text{Mn}_{2-x}\text{O}_4$ (M = (a) Mg, (b) Cu) showing two bands centered at 620 cm^{-1} and 530 cm^{-1} .

becomes longer with x ; further, the changes in the IR spectra for Mg and Zn compounds also exhibit similar phenomena. In addition, the peaks become broader with increasing x , as shown in Fig. 3 due to the diversity of cations in the octahedral sites. In the Cu compound, the position of the band at 525 cm^{-1} was shifted to lower wave numbers with x , and both peaks became broader, indicating that the Li–O bond became longer and the distribution of the cations may disturb the interaction between the cation–oxygen bonds.

Electrical Conductivity. The temperature dependence of the electrical conductivity for $\text{LiMg}_x\text{Mn}_{2-x}\text{O}_4$ is shown in Fig. 4. The conductivity for all compounds was increased with rising temperature. With increasing the Mg or Zn content, the conductivity decreased and its slope became steep. The activation energy is obtained from the equation

$$\sigma(T) = A \exp(-E_a/RT) T^{-1}, \quad (1)$$

where $\sigma(T)$ and A are the electrical conductivity and a pre-exponential parameter. By fitting (1) to the observed data, the activation energies were evaluated to be 48 kJ mol^{-1} and 67 kJ mol^{-1} for $\text{LiMg}_{0.1}\text{Mn}_{1.9}\text{O}_4$ and $\text{LiMg}_{0.5}\text{Mn}_{1.5}\text{O}_4$. Figure 5 shows plots of the electrical conductivity at 300 K (a) and the activation energy (b) against x in each compound. The conductivity in both $\text{LiMg}_x\text{Mn}_{2-x}\text{O}_4$ and $\text{LiZn}_x\text{Mn}_{2-x}\text{O}_4$ decreased from 10^{-4} S cm^{-1} to 10^{-7} S cm^{-1} and the activation energy increased with x . In Cu compounds, the conductivity changed slightly compared with Mg and Zn compounds, and the activation energies were between 42 to 45 kJ mol^{-1} . The conductivity for LiMn_2O_4 is mainly governed by the electronic conduction due to the e_g electron of the Mn^{3+} ion. The ionic conductivity for the Li ion of all compounds was very small in our experiments using an electron-blocking electrode (Li ion conduc-

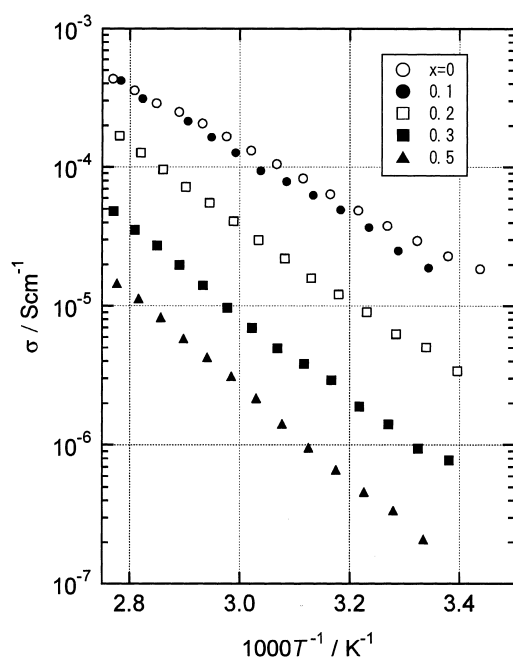


Fig. 4. Temperature dependence of electrical conductivity for $\text{LiMg}_x\text{Mn}_{2-x}\text{O}_4$ plotted against the inverse of temperature.

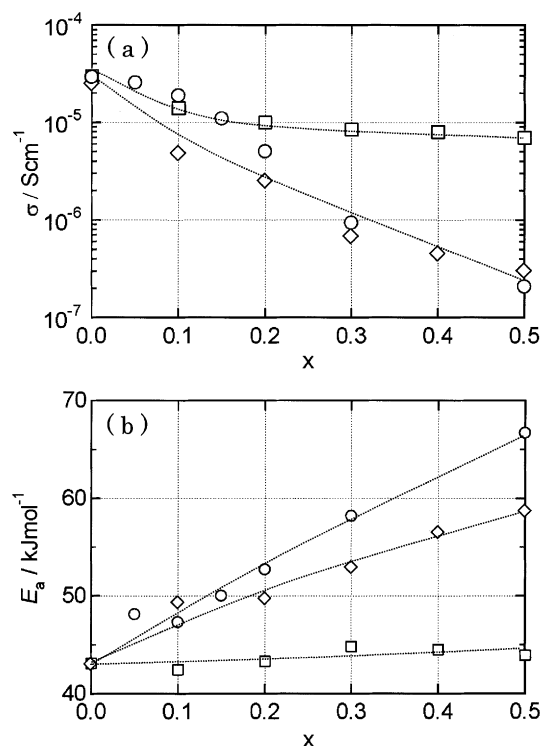


Fig. 5. x dependence of electrical conductivity (a) at 300 K and activation energy (b) for conduction in $\text{LiM}_x\text{Mn}_{2-x}\text{O}_4$ ($M = \text{Mg}$ (\circ), Zn (\diamond), and Cu (\square)). The dotted lines are for a guide.

tive glass). These results indicate that Mg and Zn substituted for Mn have no contribution to the electrical conduction but Cu for Mn contributes to the electrical conductivity in each compound. This is consistent with the result for $\text{Li}_{1-2x}\text{Cu}_x\text{Mn}_2\text{O}_4$ in our previous paper.²⁰ It was expected that the decrease in the conductivity for Mg and Zn compounds is produced by a lack of Mn(III)–O bond due to substitution for Mn. The slight decrease in the conductivity for the Cu compound may be caused by a decrease in the Mn(III)–O bond and a partial change of the Mn–O bond for the Cu–O bond.

X-ray Photoelectron Spectroscopy. Information of the oxidation state of manganese ions was obtained from the change in the XPS spectra of the $\text{Mn}2p_{3/2}$ signal. Figure 6 shows the $\text{Mn}2p_{3/2}$ spectra of LiMn_2O_4 , $\text{LiCu}_{0.5}\text{Mn}_{1.5}\text{O}_4$, $\text{LiMg}_{0.5}\text{Mn}_{1.5}\text{O}_4$ and $\text{LiZn}_{0.5}\text{Mn}_{1.5}\text{O}_4$. The spectrum for LiMn_2O_4 exhibits two components after peak deconvolution. Each component is shown in Fig. 6 by the dotted line. The peak observed at about 641.8 and 642.8 eV , whose binding energies are consistent with the binding energy for Mn^{3+} and Mn^{4+} , respectively, are given in previous literature.²¹ The peak intensity of the Mn^{3+} ion is almost the same as that of the Mn^{4+} ion in LiMn_2O_4 . For $\text{LiMg}_{0.5}\text{Mn}_{1.5}\text{O}_4$ and $\text{LiZn}_{0.5}\text{Mn}_{1.5}\text{O}_4$, each spectrum has one component corresponding to the Mn^{4+} ion. These results indicate that the oxidation states of the manganese ion in $\text{LiMg}_x\text{Mn}_{2-x}\text{O}_4$ and $\text{LiZn}_x\text{Mn}_{2-x}\text{O}_4$ are changed with Mg or Zn doping, and that all manganese ions become Mn^{4+} ion at $x = 0.5$. For $\text{LiCu}_{0.5}\text{Mn}_{1.5}\text{O}_4$, however, the $\text{Mn}2p_{3/2}$ spectrum has two components, indicating the existence of both Mn^{3+} and Mn^{4+} ions. The relative intensity of

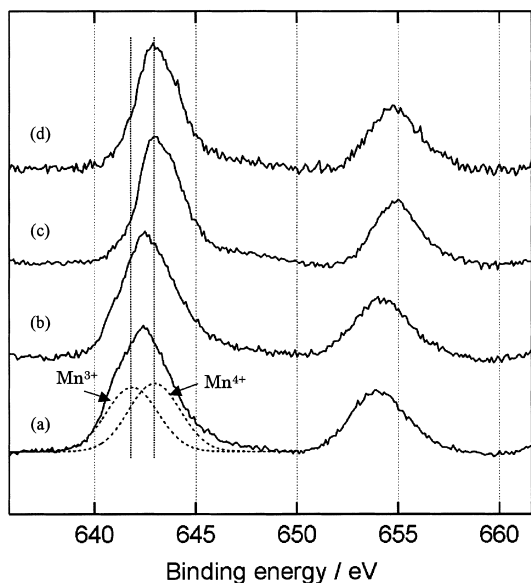


Fig. 6. XPS of the Mn 2p region for (a) LiMn_2O_4 , (b) $\text{LiCu}_{0.5}\text{Mn}_{1.5}\text{O}_4$, (c) $\text{LiZn}_{0.5}\text{Mn}_{1.5}\text{O}_4$, and (d) $\text{LiMg}_{0.5}\text{Mn}_{1.5}\text{O}_4$. The dotted lines are fitting lines for Mn^{3+} and Mn^{4+} ions after peak deconvolution.

Mn^{3+} to Mn^{4+} decreased with increasing the Cu content, indicating that the Mn^{3+} ion partially converted to Mn^{4+} ion. The existence of an impurity phase was not confirmed, and the difference in the amounts of oxygen atoms due to Cu substitution was hardly noticed. The reason for this result could not be interpreted sufficiently.

Conclusion

The lattice constants in $\text{LiM}_x\text{Mn}_{2-x}\text{O}_4$ were varied by substitution. The bond lengths were also varied by substitution in Zn and Mg compounds, and no significant difference was observed in Cu compounds. The electrical conductivity for Mg and Zn compounds decreased from $10^{-4} \text{ S cm}^{-1}$ to $10^{-7} \text{ S cm}^{-1}$. Because the conductivity for LiMn_2O_4 is mainly governed by the electronic conduction due to the Mn^{3+} ion, the decreases in the conductivity arises from a lack of the $\text{Mn(III)}\text{--O}$ bond. In the Cu compound, the conductivity did not change very much because all of the Mn^{3+} ions were not necessarily changed to Mn^{4+} ions even in $\text{LiCu}_{0.5}\text{Mn}_{1.5}\text{O}_4$, and the $\text{Mn(III)}\text{--O}$ bond may contribute to the electrical conduction.

References

- 1 T. J. Boyle, D. Ingersoll, T. M. Alam, C. J. Tafuya, M. A. Rodriguez, K. Vanheusden, and D. H. Doughty, *Chem. Mater.*, **10**, 2270 (1998).
- 2 M. Okada, K. Takahashi, and T. Mouri, *J. Power Sources*, **68**, 545 (1997).
- 3 J. Dai, S. F.Y. Li, Z. Gao, and K. S. Siow, *J. Electrochem. Soc.*, **145**, 3057 (1998).
- 4 M.M. Thackelley, W.I.F. David, P.G. Bruce, and J.B. Goodenough, *Mater. Res. Bull.*, **18**, 461 (1983).
- 5 M.M. Thackelley, A. De Kock, M.H. Rossouw, D.C. Liles, R. Bittihn, and D. Hoge, *J. Electrochem. Soc.*, **139**, 363 (1992).
- 6 Y. Xia, H. Takeshige, H. Noguchi, and M. Yoshio, *J. Power Sources*, **56**, 61 (1995).
- 7 A. De Kock, E. Ferg, and R.J. Gummow, *J. Power Sources*, **70**, 247 (1998).
- 8 K. Amine, H. Tsukamoto, H. Yasuda, and Y. Fujita, *J. Power Sources*, **68**, 604 (1997).
- 9 C. H. Shen, R. S. Liu, R. Gundakaram, J. M. Chen, S. M. Huang, J. S. Chen, and C. M. Wang, *Journal of Power Sources*, **102**, 21 (2001).
- 10 M. Okada, Y.-S. Lee, and M. Yoshio, *J. Power Sources*, **90**, 196 (2000).
- 11 E. Iguchi, N. Nakamura, and A. Aoki, *Philos. Mag. B*, **78**, 65 (1998).
- 12 F. Izumi, in "The Rietveld Method," ed by R. A. Young, Oxford University Press, Oxford (1993), p. 236.
- 13 Y. Ein-Eli, W. F. Howard, Jr., S. H. Lu, S. Mukerjee, J. McBreen, J. T. Vaughey, and M. M. Thackeray, *J. Electrochem. Soc.*, **145**, 1238 (1998).
- 14 N. Hayashi, H. Ikuta, and M. Wakihara, *J. Electrochem. Soc.*, **146**, 1351 (1999).
- 15 R. D. Shannon, *Acta Crystallogr. Sect. A*, **32**, 751 (1976).
- 16 C. Wu, Z. Wang, F. Wu, L. Chen, and X. Huang, *Solid State Ionics*, **144**, 277 (1996).
- 17 L. El-farh, M. Massot, M. Lemal, and C. Julien, *J. Electroceram.*, **3**, 425 (1999).
- 18 B. Ammundsen, G.R. Burns, M.S. Islam, H. Kanoh, and J. Ž. Roziere, *J. Phys. Chem. B*, **103**, 5175 (1999).
- 19 W. Huang, R. Frech, *Solid State Ionics*, **86–88**, 395 (1996).
- 20 Y. Tomita, K. Asai, and K. Kobayashi, *Chem Lett.*, **1999**, 1023.
- 21 B. Gillot, S. Buguet, E. Kester, C. Baubet, and Ph. Tailhades, *Thin Solid Films*, **357**, 223 (1999).